Journal of Alloys and Compounds 787 (2019) 1320–1326

Contents lists available at ScienceDirect

Journal of Alloys and Compounds

journal homepage: http://www.elsevier.com/locate/jalcom

Superplastic deformation behavior of lamellar microstructure in a hydrogenated friction stir welded Ti-6Al-4V joint

L.H. Wu [a], C.L. Jia [a], S.C. Han [a], N. Li [a], D.R. Ni [a], B.L. Xiao [a], Z.Y. Ma [a, *], M.J. Fu [b], Y.Q. Wang [b], Y.S. Zeng [b, **]

[a] Shenyang National Laboratory for Materials Science, Institute of Metal Research, Chinese Academy of Sciences, 72 Wenhua Road, Shenyang, 110016, China
[b] Avic Manufacturing Technology Institute, 1 Dongjunzhuang Road, Beijing, 100024, China

ARTICLE INFO

Article history:
Received 23 October 2018
Received in revised form
31 January 2019
Accepted 15 February 2019
Available online 16 February 2019

Keywords:
Ti alloys
Friction stir welding
Superplasticity
Hydrogenation
Globularization

ABSTRACT

It is rather difficult for Ti alloy welds to be superplastic formed due to their low superplasticity and high flow stress. In this study, the Ti-6Al-4V alloy after hydrogenation with 0.2 wt% hydrogen was subjected to friction stir welding (FSW). The superplastic behavior of the FSW joint was investigated. The stir zone with a fine lamellar microstructure exhibited a largest elongation of 660% at 825 °C and 3×10^{-3} s^{-1}. Besides, the stir zone showed a similar superplasticity of close to 600% to the base material at 825 °C, 3×10^{-4}–1×10^{-3} s^{-1}. It is the first report on the superplasticity of FSW Ti alloy joints with hydrogenation. Compared to the FSW Ti-6Al-4V alloy joint without hydrogenation, the hydrogenated FSW joint showed superior superplastic properties, including a high elongation, less than a half flow stress and lower superplastic temperature. These superior superplastic properties were mainly attributed to the globularization of the lamellar microstructure and the high fraction of β phase induced by the hydrogen element. This study provides an effective way to reduce the difficulty of practical superplastic forming for Ti alloy welds, although a dehydrogenation process is still needed to avoid hydrogen embrittlement.

1. Introduction

Ti alloys have been extensively used in the aerospace industries because of their excellent properties such as high specific strength and superior corrosion resistance [1]. However, the processing of Ti alloys is rather difficult due to their high strength at both room and high temperatures and the low thermal conductivity. Fortunately, Ti alloys usually exhibit superplastic behavior. Therefore, superplastic forming (SPF), a near-net forming technique with a low cost and good flexibility, has been widely used to fabricate Ti components [1].

Nowadays, to be larger and more integrated is gradually becoming a main developing trend for aerospace components. Therefore, it is necessary to combine SPF with joining techniques for manufacturing large-sized integrated components. Whatever joining techniques to apply, the key object is to achieve a uniform SPF in the entire weld. This requires the similar superplastic deformation ability in each zone in the weld [2]. Generally speaking, fine and equiaxed microstructure is the prerequisite for good superplasticity (SP) [3,4]. Commercially rolled Ti alloy sheets with fine microstructure show a relatively good SP. However, when they were joined by fusion welding, this superior SP would be destroyed by the coarse microstructure in the fusion welds, hindering the uniform SPF in the entire welds [5].

Friction stir welding (FSW), a solid-state joining technique, has been widely used for joining metals, metal based composites and even polymer based materials [6–9], and recently FSW of Ti alloys has especially drawn a lot of attentions [10–12]. More recently, researchers have shown great interest on the combination of FSW with SPF of Ti alloys, because FSW is a very effective welding technique to retain the superplasticity of the base materials (BM) [4,13,14], and FSW/SPF shows great potential to produce large-sized Ti components.

It is important to point out that to conduct FSW/SPF of Ti alloys is very challenging mainly because of two aspects. First, tool wear is still the main factor limiting the application of FSW for Ti alloys [15]. Second, more importantly, it is rather difficult to obtain the similar superplastic deformation ability for the FSW Ti alloy joint with the BM only via adjusting the FSW processing parameters

* Corresponding author.
** Corresponding author.
E-mail addresses: zyma@imr.ac.cn (Z.Y. Ma), yszeng@hotmail.com (Y.S. Zeng).

https://doi.org/10.1016/j.jallcom.2019.02.182
0925-8388/

[13,14].

It has been reported that in different zones of the FSW Ti alloy joint, the stir zone (SZ) is the key zone influencing the superplastic behavior of the entire FSW joint [14,16]. In most FSW parameters, the SZ consists of lamellar microstructure because the temperature during FSW usually exceeds the β transus temperature [17,18]. In our previous studies [2,16], a high SP of more than 700% was obtained at 925 °C, 3×10^{-3} s^{-1} for the lamellar microstructure in the FSW Ti-6Al-4V alloy joint. Meanwhile, the similar superplastic deformation ability could be achieved for the SZ and the BM at 800 °C, $3 \times 10^{-4}s^{-1}$. However, the maximum flow stress of the SZ at 800 °C, $3 \times 10^{-4}s^{-1}$ was ~49 MPa [2], still too high, which would largely increase the difficulty of the SPF of the joint. Therefore, in order to make the practical SPF process more easily, it is necessary to reduce the flow stress of the SZ.

Hydrogen is the temporary element in Ti, which can be solved into Ti by annealing at hydrogen atmosphere (called hydrogenation), and then totally removed by vacuum annealing. The proper solution of hydrogen reduces the flow stress of Ti [19], and thus the processing of Ti with a proper fraction of hydrogen becomes easier. It has been reported that hydrogenation could obviously reduce the tool wear during FSW of Ti alloys, and enhance the quality of the weld surface [20].

More importantly, hydrogen can adjust the superplastic deformation ability of Ti alloys [21]. It was reported that the proper hydrogen could increase the SP, reduce the superplastic temperature and the flow stress during superplastic deformation [21,22]. For example, for Ti600, a content of 0.5 wt% hydrogen in Ti could reduce the SP temperature by ~80 °C, and the flow stress reduced more than 75% [22]. Therefore, hydrogenation might be a good method to adjust the superplastic properties of FSW Ti alloy joints. However, so far, there have not been reports on the superplastic deformation behavior of FSW Ti alloy joints with hydrogenation.

In this study, the Ti-6Al-4V alloy was pretreated utilizing a hydrogenation process, and then subjected to FSW. The superplastic behavior of the SZ in the FSW hydrogenated Ti-6Al-4V alloy joint was studied. The object is: (a) to obtain a joint with a fine lamellar microstructure for achieving a superior SP and low flow stress, and (b) to clarify the superplastic deformation mechanism of the FSW hydrogenated Ti-6Al-4V alloy.

2. Experimental material and methods

The as-received material was 2-mm-thick mill-annealed Ti–6Al–4V sheet. Before FSW, the Ti–6Al–4V sheet was hydrogenated at 750 °C for 2 h at pure hydrogen atmosphere. The actual content of hydrogen in the Ti–6Al–4V sheet was 0.2 wt%, determined by Hydrogen/Nitrogen/Oxygen Analyzer (LECO TCH600).

FSW was conducted in the single hydrogenated Ti–6Al–4V alloy sheet at a rotation rate of 400 rpm and a transverse speed of 100 mm/min. A W-25Re alloy welding tool was used, which consisted of a concave shoulder 11 mm in diameter and a pin tapered from 6.4 mm diameter at the root to 4.5 mm diameter at the tip, with a length of 1.6 mm.

Microstructural characterization was carried out by optical microscopy (OM, Zeiss Axio Observer Z1) and transmission electron microscopy (TEM, FEI Tecnai $G^2$20). Specimens for TEM were prepared by twin-jet electropolishing with a solution of 6 vol% $HClO_4$ + 34 vol% CH_3OH + 60 vol% C_4H_9OH at the voltage of 11 V and at the temperature range from −25 °C to −30 °C. The phase constituents were identified by X-ray diffraction (XRD, Smartlab) using Cu Ka radiation.

Dogbone-shaped tensile specimens with a gauge length of 2.5 mm and a width of 1.4 mm were cut from the SZ of the FSW joint, parallel to the welding plate plane. Constant crosshead speed tensile tests were carried out on an Instron 5848 micro-tester. To prevent from oxidization, the tensile specimens were coated with antioxidant protective coating (K01 commercial antioxidant protective coating). The specimens were installed at room temperature, and then they were heated in the furnace until to the superplastic test temperature. To reach thermal equilibrium, each specimen was held at the testing temperature for 5 min before tension. The specimens for superplastic deformation were tested at the temperature range of 700–900 °C and at strain rates of $1 \times 10^{-4}s^{-1}$–$1 \times 10^{-2}s^{-1}$. Specimens after tension were cooled rapidly in water to keep the microstructure information just after tension.

3. Results and discussion

Fig. 1 shows the XRD results of the hydrogenated Ti-6Al-4V BM and the SZ of the FSW joint. It shows that the BM consisted of hexagonal close packed (HCP) α phase, body centered cubic (BCC) β phase and a small fraction of γ and δ hydride phases. The γ hydride phase is TiH phase, with a tetragonal lattice structure (c = 0.4576 nm and a = 0.4199 nm; c:a = 1.09) [23–25]. The δ hydride phase is TiH_2 phase, with a FCC structure (a = 0.445 nm) [23,24]. After FSW, the δ hydride phase was not detected by XRD, and the fraction of β phase decreased. Compared to the BM, the diffraction pattern of the HCP phase in the SZ had a degree of broadening. It is well-known that the lamellar HCP α and martensitic α phases have the similar HCP structure and lattice parameter. Thus, their XRD patterns are almost overlapped, and the concurrent existing of these two phases would result in a broadening of their XRD patterns [26]. Therefore, the SZ consisted of α and α′ martensite phases, β phase and a small fraction of γ hydride phase.

The microstructures of the hydrogenated Ti-6Al-4V BM and SZ are shown in Fig. 2. The BM consisted of equiaxed α, the transformed β (transformed from the high temperature β phase) and a small fraction of black phases (Fig. 2a). These black phases should be titanium hydride phases (δ and γ phases) inferred from the XRD result. The SZ consisted of a very fine lamellar microstructure (Fig. 2b), which suggested that the welding temperature was over the β transus, and that the materials in the SZ experienced a rapid cooling process after FSW. TEM images (Fig. 2c) indicated that there were two types of lamellar or acicular phases. One is the main lamellar structure (100–500 nm in thickness) precipitated from the matrix. Combined the morphology and XRD result, they were determined as HCP α and α′ martensite phases. It was reported that a fully α′ martensite microstructure was formed under a very fast

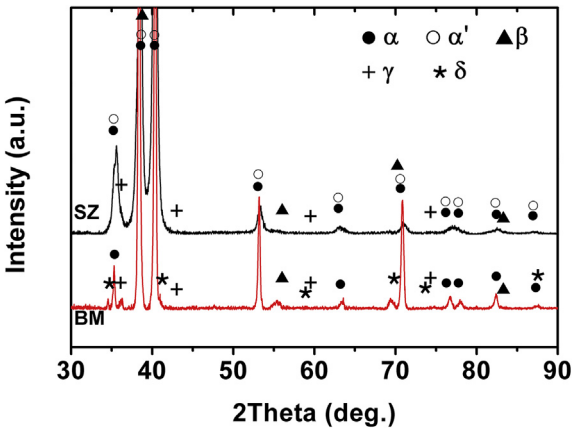

Fig. 1. XRD result of hydrogenated Ti-6Al-4V BM and SZ in FSW joint.

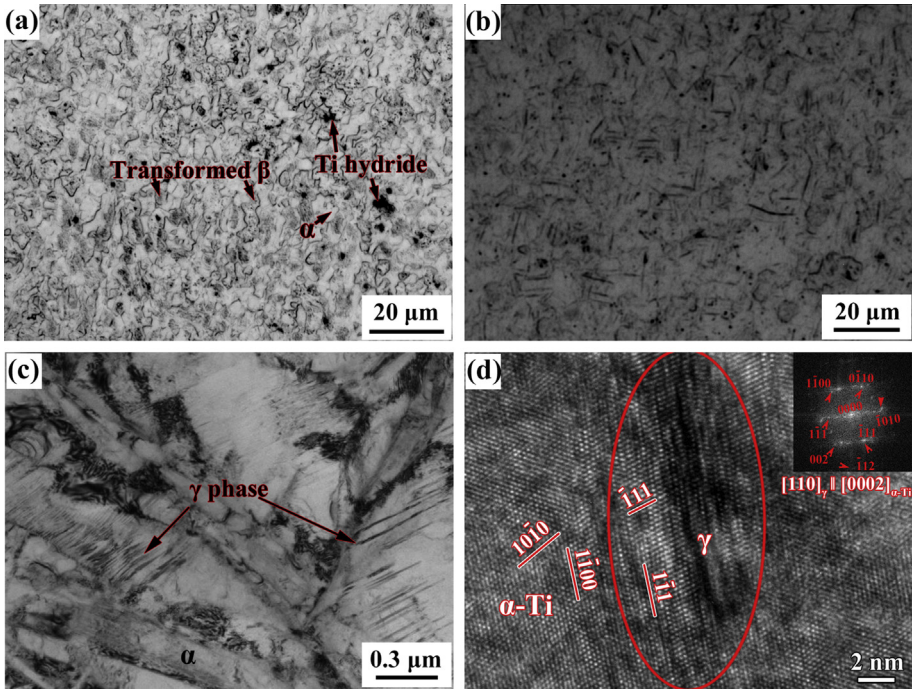

Fig. 2. Microstructure of hydrogenated Ti-6Al-4V alloy: (a) (b) OM of BM and SZ, (c) (d) TEM and high resolution TEM images of SZ. In (d), a Fast Fourier Transform from high resolution TEM was inserted.

cooling rate of >410 °C [27]. Although a fast cooling took place after FSW, it was still very difficult to achieve such a high cooling rate for the air cooling condition. Thus, both α and α′ martensite phases existed in the SZ.

The other is nano-scaled acicular structure (10–20 nm in thickness) parallel-arranged in the α or α′ lamellae. These parallel nano-scaled acicular phases were determined as γ phases by high resolution TEM and its Fast Fourier Transform (Fig. 2d). From Fig. 2d, the γ hydride phase formed as acicular plates with a {10-10} habit plane, and the <110> direction of the γ hydride phase was parallel to the <0002> direction of the α-Ti phase.

It was reported that γ phase was a metastable phase at a high temperature, which was formed at a low hydrogen content, and when the hydrogen content increased, γ phase disappeared [23,24]. The formation of the δ phase passed through the formation of the intermediate, metastable γ phase at 400–600 °C [21,23]. In the hydrogenated Ti-6Al-4V BM in this study, the content of hydrogen did not reach the critical content for the formation of the γ phase and δ phase [23]. The formation of these two titanium hydride phases might be attributed to the segregation of the hydrogen atoms during hydrogenation. During FSW, due to the "stirring" effect, the segregation extent of the hydrogen atoms might decrease, and thus the δ phase almost disappeared. However, the detailed formation process of hydrides still needs to be studied further, which is beyond the scope of this study, and will not be discussed deeply in this study.

The content of hydrogen in the SZ was 0.2 wt% determined by the Hydrogen/Nitrogen/Oxygen Analyzer (not shown), the same as that for the hydrogenated Ti–6Al–4V BM. This suggests that FSW hardly affect the content of hydrogen in the Ti-6Al-4V alloy. It was reported that when the hydrogenated Ti alloys was treated at high temperature at vacuum or Ar atmosphere vacuum, hydrogen would escape from Ti alloys [28]. In this study, the content of hydrogen hardly decreased, which should be attributed to a very short duration at the high temperature during FSW, and the hydrogen element hardly escaped from the joint.

The superplastic behaviors of the SZ and the BM in the FSW hydrogenated Ti–6Al–4V alloy joint are shown in Fig. 3. For simplification, the SZ in the FSW hydrogenated Ti–6Al–4V alloy joint was called the H-FSW specimen in the following part. When the strain rate was 1×10^{-3} s^{-1}, with the temperature increasing, the elongation first increased, and then decreased. A maximum elongation of 600% was achieved at 825 °C and 1×10^{-3} s^{-1} (Fig. 3a). In order to obtain the optimum strain rate, the elongations at different strain rates at the temperature range of 800–850 °C for the H-FSW specimen were measured, as shown in Fig. 3b. At all the temperatures of 800–850 °C, the elongation first increased and then decreased with the strain rate increasing. The maximum elongation of 660% was achieved at 825 °C and 3×10^{-3} s^{-1}. Obviously, the optimum superplastic deformation temperature in this study was 825 °C. In our previous study [16], the optimum superplastic deformation temperature for the SZ of the FSW Ti-6Al-4V alloy joint without hydrogenation was 925 °C. Therefore, hydrogenation could reduce the optimum superplastic temperature by 100 °C.

For comparison, the variation of SP with the initial strain rate for the hydrogenated Ti-6Al-4V BM is shown in Fig. 3c. It was found that at 825 °C, $3 \times 10^{-4}s^{-1}$ –$1 \times 10^{-3}s^{-1}$, the SZ showed a comparable SP of close to 600% with the BM. It is of great significance since this means that a superior SP in the entire joint could be obtained without the local low-SP zone.

The stress-strain curves at different strain rates at 800 °C for the H-FSW specimen are shown in Fig. 4a (red dash dot lines). At $1 \times 10^{-3}s^{-1}$, the flow stress first increased, and then exhibited a decreasing trend. At $3 \times 10^{-4}s^{-1}$, the flow stress first increased, then exhibited an almost steady-state flow trend until ~0.8, and finally showed a continuous increasing trend. At the intermedium strain region of ~0.2–0.8, an almost steady flow stress was the typical characteristic when grain or phase boundary sliding (GBS/PBS) dominated the deformation [16,29]. At the last stage, the continuous increase of flow stress was the typical result of grain coarsening during superplastic deformation [29]. Therefore, for the

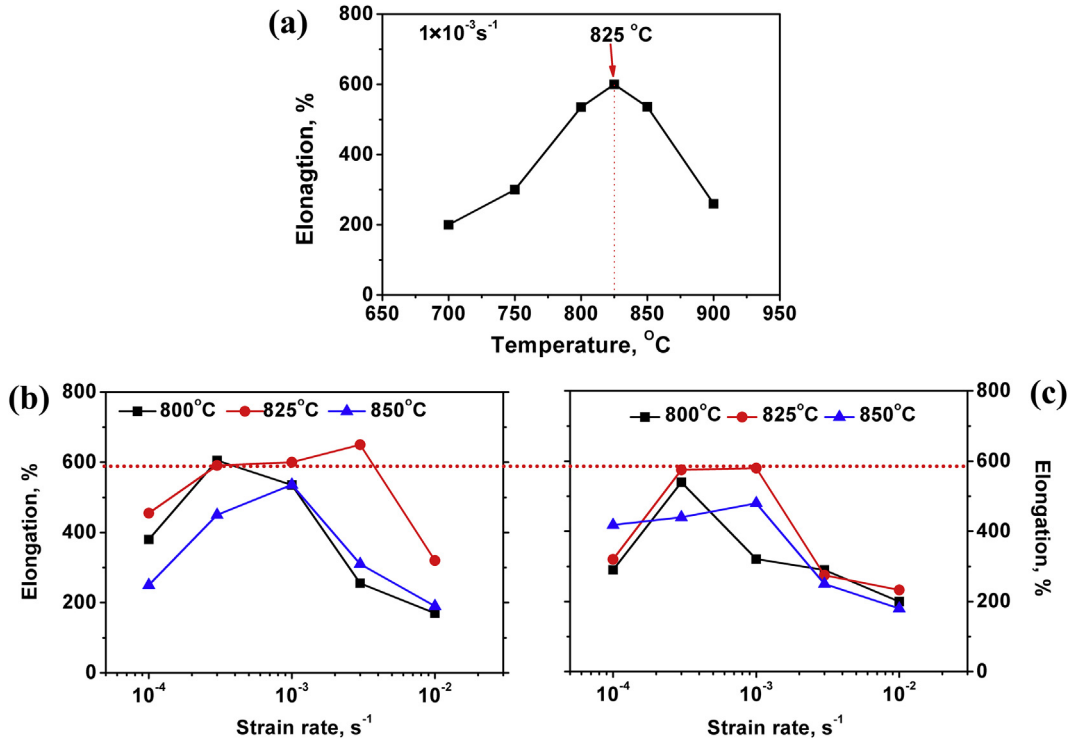

Fig. 3. Superplastic behavior of SZ in FSW hydrogenated Ti-6Al-4V alloy joint: variation of elongation with (a) temperature at 1×10^{-3} s^{-1} and (b) initial strain rate at 800–850 °C; and (c) initial strain rate for hydrogenated Ti-6Al-4V BM.

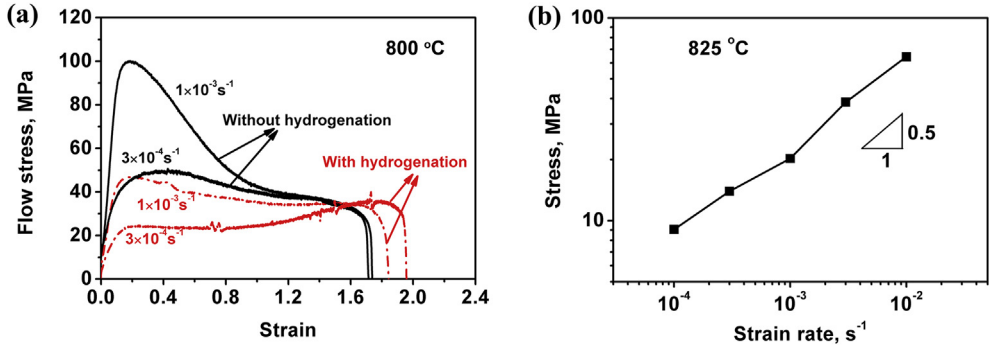

Fig. 4. (a) True stress-true strain curves at 800 °C, 1×10^{-3} and 3×10^{-4} s^{-1} (red dash dot lines), (b) variation of flow stress with initial strain rate at 825 °C for SZ in FSW hydrogenated Ti-6Al-4V alloy joint. For comparison, the true stress-strain curves of the SZ in the FSW Ti-6Al-4V joint without hydrogenation were overlapped in (a) (black solid lines) [2]. (For interpretation of the references to colour in this figure legend, the reader is referred to the Web version of this article.)

H-FSW specimen, the main superplastic deformation mechanism might be related to GBS/PBS.

For comparison, the data obtained at 800 °C for the SZ of the FSW joint without hydrogenation (called as the FSW specimen) is also shown in Fig. 4a (black solid lines) [2]. It was obvious that the H-FSW specimen showed a much lower stress for both the strain rates. For the FSW specimen, the flow stress ($\varepsilon = 0.1\%$) at 800 °C, $1 \times 10^{-3}s^{-1}$ was 75.8 MPa. However, for the H-FSW specimen, the flow stress was only 33.6 MPa, more than a half lower than that of the FSW specimen. At 3×10^{-4} s^{-1}, hydrogenation also reduced the flow stress more than a half, from 30.2 MPa to 12.2 MPa. Therefore, hydrogenation before FSW was beneficial to reduce the difficulty of SPF via the large decrease of flow stress, thereby decreasing the forming cost.

The variation of flow stress with initial strain rate at 825 °C for the H-FSW specimen is shown in Fig. 4b. The strain rate sensitivity *m* value was ~0.5. It was reported that when the *m* value was more than 0.3, the main deformation mechanism was usually related to GBS/PBS [2]. Combining the result of stress-strain curve with the *m* value, it was inferred that GBS/PBS should the main superplastic deformation mechanism of the H-FSW specimen.

Fig. 5 shows the macrostructure of tensile specimens pulled to failure at 825 °C at different strain rates. At all the strain rates, the specimens showed a relatively uniform deformation characteristic, which was the feature when GBS/PBS dominated the superplastic deformation. Therefore, it further confirmed that the main deformation mechanism for the H-FSW specimen was GBS/PBS.

The microstructures at the different regions of the H-FSW specimen after failure at 825 °C and $3 \times 10^{-3}s^{-1}$ are shown in Fig. 6. After failure, at the grip section (point B in Fig. 6a), the microstructure still consisted of lamellae although the lamellae were coarsened along the thickness direction (Fig. 6b). At the

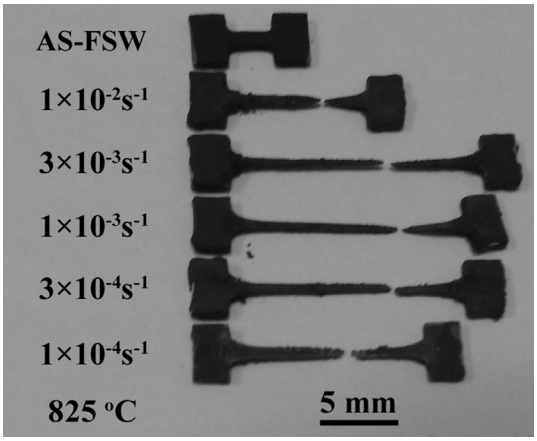

Fig. 5. Tensile specimens pulled to failure at 825 °C at different strain rates.

deformation section near the grip section (point C in Fig. 6a), some lamellae were transformed to globular grains (Fig. 6c). At the uniform deformation section (point D in Fig. 6a), the majority of lamellae were globularized (Fig. 6d). Approaching the tip (point E in Fig. 6a), a fully equiaxed and coarse microstructure exhibited (Fig. 6e). It means that as the deformation increased, the extent of globularization increased. As we know, an equiaxed microstructure promoted the superplastic deformation compared to the lamellar microstructure. Therefore, the superior SP should be related to the globularization of the lamellar microstructure.

In order to further clarify the reason for the superior superplastic properties of the H-FSW specimen, the microstructures near the tip of the tensile specimens after failure at 825 °C and $1 \times 10^{-3}s^{-1}$ for both the FSW and H-FSW specimens were observed, as shown in Fig. 7. After fracture, the H-FSW specimen consisted of fine equiaxed α grains and larger-sized grains consisting of acicular secondary α microstructure. These acicular secondary α should be transformed from the β phases during cooling, and the larger grain consisting of the acicular secondary α was called as the transformed β (β_T, marked by black lines in Fig. 7a). Thus, the fraction of the β phase at the high temperature during superplastic deformation could be described by that of β_T in Fig. 7a. For the FSW specimen, only a small fraction of β phase was distributed at the grain boundaries of equiaxed α (Fig. 7b).

Therefore, compared to the FSW specimen, the H-FSW specimen obviously exhibited a higher fraction of β phase at high temperature during superplastic deformation (Fig. 7). It should be attributed to the effect of the hydrogen element. As we know, hydrogen was a β stability element, and the solution of hydrogen in Ti alloys could reduce the β transus temperature and increase the fraction of β phase at the same temperature. Thus, the H-FSW specimen showed an obvious higher fraction of β phase at the same high temperature.

As is mentioned above, the H-FSW specimen showed superior superplastic properties including a high SP, a low flow stress and low superplastic temperatures, which should be attributed to the easy globularization of the lamellae and the high fraction of β phase induced by the hydrogen element. Especially, compared to the FSW specimen, the H-FSW specimen showed a much lower flow stress and optimum superplastic temperature, which should result from the higher fraction of β phase induced by the hydrogen element.

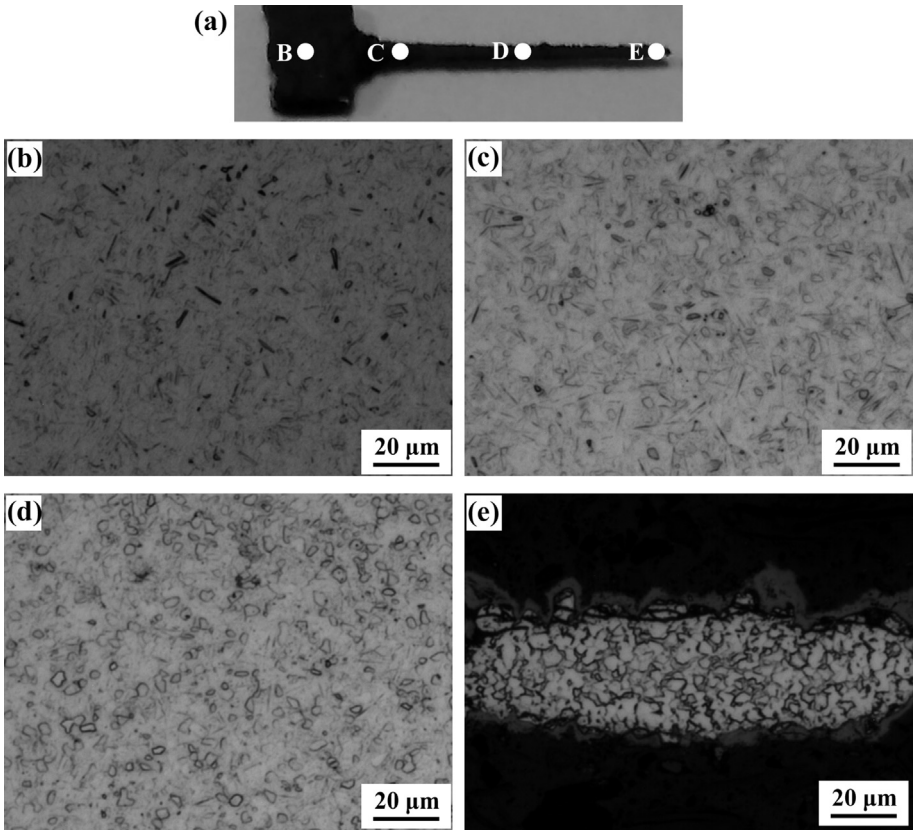

Fig. 6. Microstructures of different regions for the fracture tensile specimen at 825 °C and $3 \times 10^{-3}s^{-1}$: (a) macrostructure morphology, (b) microstructure of grip section corresponding to point B in (a), (c) microstructure of gauge section corresponding to point C in (a), (d) microstructure of gauge section corresponding to point D in (a), and (e) microstructure of gauge section corresponding to point E in (a).

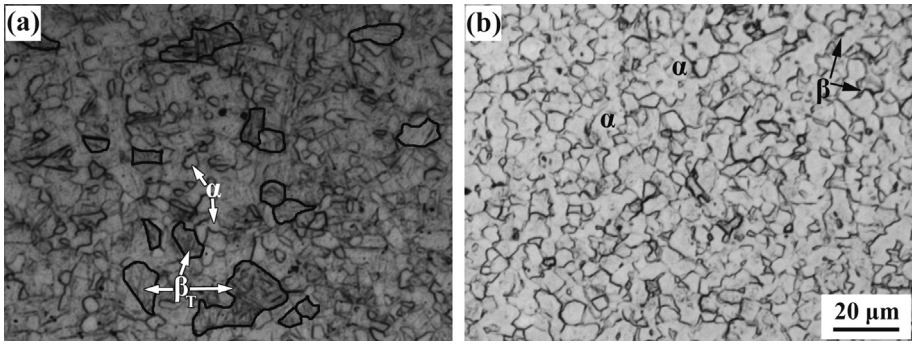

Fig. 7. Microstructure of SZ after being pulled to failure at 825 °C and $1 \times 10^{-3}s^{-1}$ for: (a) with and (b) without hydrogenation. β_T in (a) represented the transformed β.

Firstly, for the Ti-6Al-4V alloy without hydrogenation, when cooling from the β single phase field, the lamellar α phases precipitate from the β matrix, and these two phases obey a Burgers' orientation relationship. As a result, the energy of the α/β phase boundary is very low. It means that the lamellar α/β phase boundary is rather stable, and the Burgers' orientation relationship is difficult to break only by annealing. Thus, the spheriodization of lamellae is difficult to achieve only by annealing [1]. However, the content of hydrogen solved in the β phase was much larger than that in the α phase, which would result in the different distortions of lattice for the two phases [21]. As a result, the Burgers' orientation relationship between two phases was influenced, and the energies of the phase boundaries were increased. It means that the spheriodization of the lamellae during annealing and superplastic deformation was relatively easy. Therefore, in this study, hydrogen induced the globularization of the lamellae, which promoted the superplastic deformation.

Secondly, it was reported that for the Ti-6Al-4V alloy, β phase had a diffusivity ~100 times faster than α phase at the superplastic temperature, and the increase of β phases enhanced the superplasticity [30]. When the ratio of β phase and α phase was approximately 1:1, a maximum SP could be achieved, and this ratio was usually reached at 900–925 °C [30]. For the FSW specimen, the ratio of β phase and α phase was much smaller than 1:1 at the temperatures less than 850 °C (Fig. 7b). The solution of the hydrogen component resulted in the decrease of β phase transus, which increased the ratio of β phase and α phase at the same temperature (Fig. 7a). It means that the ratio of β phase and α phase could reach 1:1 at a lower temperature, and thus a superior SP could be exhibited at a lower temperature.

Lastly, β phase at high temperature was softer than α phase, and the distribution of β phases at the α grain boundaries weakened the grain boundaries [28,31]. It means that when the fraction of β phases increases, the resistance for the grain boundary sliding is reduced. Thus, the increase of β phases induced by the hydrogen element promoted the superplastic deformation and reduced the flow stress.

In summary, the globularization of the lamellae and the high fraction of β phase induced by the hydrogen element were the main reasons for the superior SP, low flow stress and superplastic temperature. It should be pointed out that the SP was likely deteriorated by the titanium hydride at high temperature [22]. In this study, although the γ hydride phase existed in the H-FSW specimen, it was reported to be decomposed in the temperature range of 400–750 °C [28], and thus at the superplastic temperature of 750–900 °C, the hydride phase would hardly deteriorate the SP of the H-FSW specimen.

It should be also pointed out that although hydrogenation in this study could increase the superplastic properties of the Ti alloy joint, which would reduce the difficulty of the practical SPF process, the remaining of H atoms in Ti would lead to "hydrogen embrittlement". Therefore, a dehydrogenation treatment by vacuum annealing after SPF was necessary, which might make the microstructure and mechanical properties of the products change, and also increase the cost of practical SPF. However, the influence of the dehydrogenation process on the microstructure and properties of superplastic specimens still need more investigations in the future.

4. Conclusions

In this study, the superplastic behavior of the FSW Ti alloy joints with hydrogenation was reported for the first time. The following conclusions are reached.

1. The fine lamellar microstructure in the SZ exhibited a largest elongation of 660% at 825 °C and 3×10^{-3} s^{-1}. Besides, the SZ showed a similar SP of close to 600% to the BM at 825 °C, 3×10^{-4}–1×10^{-3} s^{-1}.
2. Compared to the FSW Ti-6Al-4V alloy joint without hydrogenation, the hydrogenated FSW joint showed a superior SP, less than a half flow stress and 100 °C lower superplastic temperature.
3. The superior superplastic properties of the SZ were mainly related to the easy globularization of the lamellae and the high fraction of β phase induced by the hydrogen element.

Declarations of interest

None.

Acknowledgement

This work was supported by the National Natural Science Foundation of China under Grant Nos. 51601194, 51471171, 51331008 and the IMR SYNL-T.S. Kê Research Fellowship.

Appendix A. Supplementary data

Supplementary data related to this article can be found at https://doi.org/10.1016/j.jallcom.2019.02.182.

References

[1] G. Lütjering, J.C. Williams, Titanium, second ed., Springer, New York, 2007.
[2] L.H. Wu, P. Xue, B.L. Xiao, Z.Y. Ma, Achieving superior low-temperature superplasticity for lamellar microstructure in nugget of a friction stir welded Ti-6Al-4V joint, Scripta Mater. 122 (2016) 26–30.
[3] F.C. Liu, Z.Y. Ma, Achieving exceptionally high superplasticity at high strain

rates in a micrograined Al-Mg-Sc alloy produced by friction stir processing, Scripta Mater. 59 (2008) 882–885.
[4] L.H. Wu, H. Zhang, X.H. Zeng, P. Xue, B.L. Xiao, Z.Y. Ma, Achieving superior low temperature and high strain rate superplasticity in submerged friction stir welded Ti-6Al-4V alloy, Sci. China Mater. 61 (2018) 417–423.
[5] A.A. Kruglov, F.U. Enikeev, R.Y. Lutfullin, Superplastic forming of a spherical shell out a welded envelope, Mater. Sci. Eng. A 323 (2002) 416–426.
[6] L.H. Wu, K. Nagatsuka, K. Nakata, Achieving superior mechanical properties in friction lap joints of copper to carbon-fiber-reinforced plastic by tool offsetting, J. Mater. Sci. Technol. 34 (2018) 1628–1637.
[7] N.Z. Khan, A.N. Siddiquee, Z.A. Khan, A.K. Mukhopadhyay, Mechanical and microstructural behavior of friction stir welded similar and dissimilar sheets of AA2219 and AA7475 aluminium alloys, J. Alloy. Comp. 695 (2017) 2902–2908.
[8] H.B.M. Rajan, I. Dinaharan, S. Ramabalan, E.T. Akinlabi, Influence of friction stir processing on microstructure and properties of AA7075/TiB2 in situ composite, J. Alloy. Comp. 657 (2016) 250–260.
[9] L.H. Wu, K. Nagatsuka, K. Nakata, Direct joining of oxygen-free copper and carbon-fiber-reinforced plastic by friction lap joining, J. Mater. Sci. Technol. 34 (2018) 192–197.
[10] L.H. Wu, D. Wang, B.L. Xiao, Z.Y. Ma, Microstructural evolution of the thermomechanically affected zone in a Ti-6Al-4V friction stir welded joint, Scripta Mater. 78–79 (2014) 17–20.
[11] M. Ramulu, P.D. Edwards, D.G. Sanders, A.P. Reynolds, T. Trapp, Tensile properties of friction stir welded and friction stir welded-superplastically formed Ti-6Al-4V butt joints, Mater. Des. 31 (2010) 3056–3061.
[12] L.H. Wu, X.B. Hu, X.X. Zhang, Y.Z. Li, Z.Y. Ma, X.L. Ma, B.L. Xiao, Fabrication of high-quality Ti joint with ultrafine grains using submerged friction stirring technology and its microstructural evolution mechanism, Acta Mater. 166 (2019) 371–385.
[13] D.G. Sanders, M. Ramulu, P.D. Edwards, A. Cantrell, Effects on the surface texture, superplastic forming, and fatigue performance of titanium 6AL-4V friction stir welds, J. Mater. Eng. Perform. 19 (2010) 503–509.
[14] P. Edwards, M. Ramulu, Effect of process conditions on superplastic forming behaviour in Ti-6Al-4V friction stir welds, Sci. Technol. Weld. Join. 14 (2009) 669–680.
[15] L.H. Wu, D. Wang, B.L. Xiao, Z.Y. Ma, Tool wear and its effect on microstructure and properties of friction stir processed Ti-6Al-4V, Mater. Chem. Phys. 146 (2014) 512–522.
[16] L.H. Wu, B.L. Xiao, D.R. Ni, Z.Y. Ma, X.H. Li, M.J. Fu, Y.S. Zeng, Achieving superior superplasticity from lamellar microstructure of a nugget in a friction-stir-welded Ti-6Al-4V joint, Scripta Mater. 98 (2015) 44–47.
[17] A.L. Pilchak, W. Tang, H. Sahiner, A.P. Reynolds, J.C. Williams, Microstructure evolution during friction stir welding of mill-annealed Ti-6Al-4V, Metall. Mater. Trans. 42 (2011) 745–762.
[18] Y. Zhang, Y.S. Sato, H. Kokawa, S.H.C. Park, S. Hirano, Microstructural characteristics and mechanical properties of Ti-6Al-4V friction stir welds, Mater. Sci. Eng. A 485 (2008) 448–455.
[19] Y.Y. Zong, Y.C. Liang, Z.W. Yin, D.B. Shan, Effects of hydrogen addition on the high temperature deformation behavior of TC21 titanium alloy, Int. J. Hydrog. Energy 37 (2012) 13631–13637.
[20] L. Zhou, H.J. Liu, Effect of 0.3 wt% hydrogen addition on the friction stir welding characteristics of Ti-6Al-4V alloy and mechanism of hydrogen-induced effect, Int. J. Hydrog. Energy 35 (2010) 8733–8741.
[21] X. Li, J. Jiang, S. Wang, J. Chen, Y. Wang, Effect of hydrogen on the microstructure and superplasticity of Ti-55 alloy, Int. J. Hydrog. Energy 42 (2017) 6338–6349.
[22] S.Q. Zhang, L.R. Zhao, Effect of hydrogen on the superplasticity and microstructure of Ti-6Al-4V alloy, J. Alloy. Comp. 218 (1995) 233–236.
[23] D.V. Schur, S.Y. Zaginaichenko, V.M. Adejev, V.B. Voitovich, A.A. Lyashenko, V.I. Trefilov, Phase transformations in titanium hydrides, Int. J. Hydrog. Energy 21 (1996) 1121–1124.
[24] C.B. Zhang, Q. Kang, Z.H. Lai, R. Ji, The microstructural modification, lattice defects and mechanical properties of hydrogenated dehydrogenated alpha-Ti, Acta Mater. 44 (1996) 1077–1084.
[25] H. Numakura, M. Koiwa, H. Asano, F. Izumi, Neutron-diffraction study of the metastale gamma-titanium deuteride, Acta Metall. 36 (1988) 2267–2273.
[26] M.G. Glavicic, S.L. Semiatin, X-ray line-broadening investigation of deformation during hot rolling of Ti-6Al-4V with a colony-alpha microstructure, Acta Mater. 54 (2006) 5337–5347.
[27] T. Ahmed, H.J. Rack, Phase transformations during cooling in $\alpha + \beta$ titanium alloys, Mater. Sci. Eng. A243 (1998) 206–211.
[28] X. Li, N. Chen, J. Chen, Q. Mei, L. Wan, C. Jia, H. Liu, Superplastic deformation behavior of Ti-55 alloy without and with 0.1 wt% H addition, Mater. Sci. Eng. A 704 (2017) 386–390.
[29] R.S. Mishra, T.R. Bieler, A.K. Mukherjee, Overview NO-119- superplasticity in powder-metallurgy aluminum-alloys and composites, Acta Metall. Mater. 43 (1995) 877–891.
[30] M.L. Meier, D.R. Lesuer, A.K. Mukherjee, Alpha-grain size and beta-volume fraction aspects of the superplasticity of Ti-6Al-4V, Mater. Sci. Eng. A 136 (1991) 71–78.
[31] H. Yoshimura, J. Nakahigashi, Ultra-fine-grain refinement and superplasticity of titanium alloys obtained through protium treatment, Int. J. Hydrog. Energy 27 (2002) 769–774.